Mem. S.A.It. Vol. 83, 132

Memorie della

Inner disc reflection and AGN accretion states

AGN review

Th. Boller

Max-Planck-Institute für extraterrestrische Physik, PSF 1312, 85741 Garching, Germany
e-mail: bol@mpe.mpg.de

Abstract. This review concentrates on two topics, (i) are the X-ray spectra of AGN best described by the inner disc reflection model or by a distant reflector with absorption, and, (ii) AGN accretion states and their relation to Comptonized outflows. For the first topic we argue that at least for the prototype AGNs 1H 0707–495 and IRAS 13224–3809 the inner disc reflection model of Ross & Fabian (2005) provide a solid and physical description of their X-ray spectra. The second topics shows how the AGN accretion states relate to the parameters of the Comptonized outflows, which provides a plausible explanation for the global X-ray Baldwin effect.

Key words. Galaxies: active – Galaxies: observations

1. Inner disc reflection or distant reflection and absorption

1.1. The relativistic reflection model

The reflection model of (Ross & Fabian 2005) provides the most advanced reflection model for fitting AGN spectra over a large energy range from about 0.1 up to 100 keV. In the spectral fitting the emissivity index, the inner radius, the ionization parameter, the normalization of the power law and reflection component, the inclination and the Fe to solar ratio are free parameters and can be constrained with high precision in high signal-to-noise AGN spectra. XMM-Newton observations have decomposed the X-ray spectra into a strong, relativistically blurred reflection plus power law component (Miniutti & Fabian 2004), (Crummy et al. 2006), (Fabian et al. 2009), or (Ponti et al. 2009). The key observational fact revealed by XMM-Newton was the detection of a sharp spectral drop at around 7 keV in 1H 0707–495 (Boller et al. 2002), (Gallo et al. 2004) and at around 8.5 keV in IRAS 13224–3809 (Boller et al. 2003). While a partial covering interpretation, e.g. (Boller et al. 2002) results into statistically acceptable spectral fits, the relativistic reflection model provides a more physical interpretation of the spectral and timing properties (Fabian et al. 2009). The relativistic reflection model requires that the inner radius of the accretion disc is very close to a rapidly spinning black hole, results into strong light bending effects and strong variability in the power law component compared to the reflection component. The model is further supported by the presence of a 30 s time delay between the soft (less than 1 keV) and hard (greater than 1 keV) light curves detected in 1H 0707-495 (Fabian

Send offprint requests to: Th. Boller

et al. 2009). While the steep emissivity indices arising from the spectral fitting with values up to about 8, much higher than that expected from the standard Shakura-Sunyaev disc, were sometimes questioned in terms of their physical relevance, (Wilkins & Fabian 2011) have recently determined the X-ray reflection emissivity profile of 1H 0707-495 via general relativistic ray-tracing simulations. In their paper they show that the emissivity values might be as steep as observed at distances very close to the central black hole with a flattening at larger radii. The relativistic reflection model is now a powerful tool with which to study the inner workings of the ultimate powerhouse in the Universe, the accreting black hole.

1.2. Comparison with observations

1.2.1. The ”missing” response of the Fe K line strength to increasing illumination

Before the launch of XMM-Newton observations of the Fe Kα line showed the line strength was not responding to an increase of the illumination strength. This puzzle is solved with the relativistic reflection model when considering relativistic effects close to the central black hole. Fig. 1 illustrates the change of the flux of the power law and reflection component as a function of the scale height of the compact power law emitting source above the black hole ((Miniutti & Fabian 2004)). The power law component varies by a factor of about 70, while the reflection component varies only by a factor of about 4. For a given scale height of the compact source, the ratio between both model components can be calculated which results in the dependence of the Fe Kα line strength on the power law component shown in Fig. 2. The figure can be divided into three parts. At low values of the power law flux, the strength of the Fe K line is increasing (regime I). When the power law flux is further increasing the strength of the Fe K line remains constant, in agreement with the observations (regime II), while for the largest values for the power law flux, the strength of the Fe K line is even decreasing (regime III).

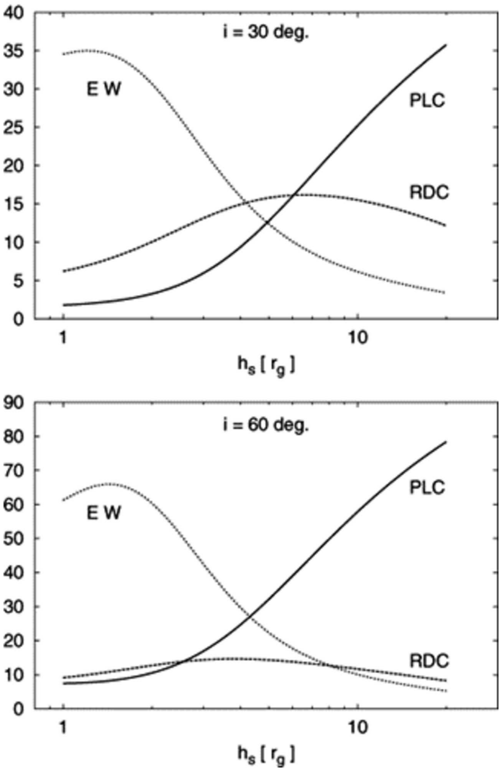

Fig. 1. The iron line EW, the reflection component, the equivalent widths of the Fe K line and the power law componentas a function of the height h. The top panel refers to an observer inclination of 30 degrees while the bottom panel is for an inclination of 60 degrees ((Miniutti & Fabian 2004), their Fig. 1, John Wiley and Sons License Number 2900730758700).

1.2.2. Spectral changes in dependence of AGN flux states

Recent observations of AGNs in different flux states revealed the presence of spectral variability. Especially the strength of the Fe Kα line is large when the source is in a low flux state. This dependence is a natural consequence of the relativistic reflection model. When the source is in the low flux state, the spectrum is dominated by the reflection component as most of the power law photons are bend towards the black hole. Therefore, the relativistic Fe K line is the dominant relativistic feature in the spectrum. When the source flux is increasing the power law component is also

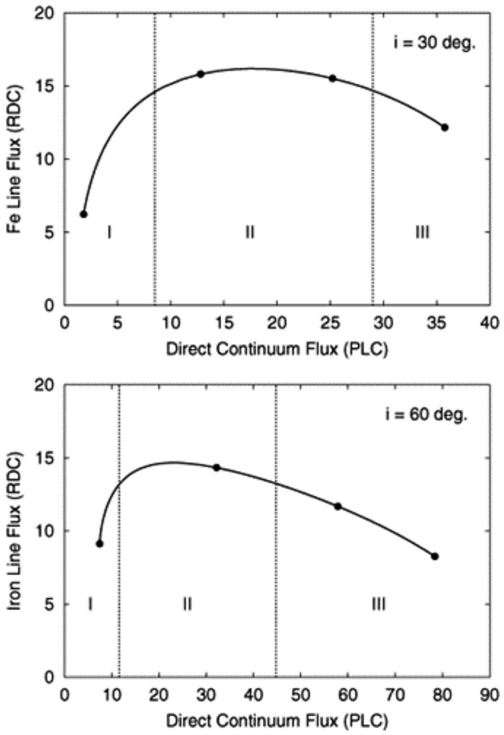

Fig. 2. Flux of the Fe Kα line as a function of the illumination strength of the power law component in the relativistic reflection model. The missing response of the strength of the Fe Kα line to the strength of the power law is explained by strong relativistic effects very close to the central black hole. ((Miniutti & Fabian 2004), their Fig. 2, John Wiley and Sons License Number 2900730758700).

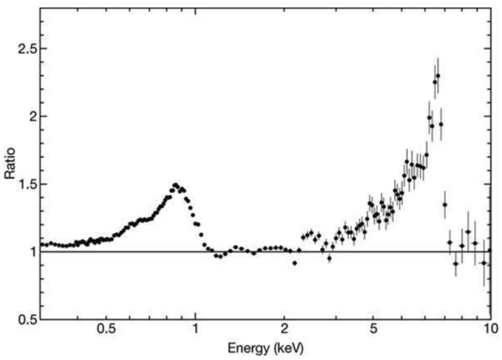

Fig. 3. Detection of both Fe K and Fe L lines in 1H 0707–495 ((Fabian et al. 2009), their Fig. 1). The ratio of the data to a simple power law and a black body model is shown (Nature License Number 2900680198102).

increasing and in the total spectrum the relativistic Fe K line is dimishing. The theoretical prediction are in excellent agreement with the observations (c.f. Fig. 12 and 13 of (Vaughan & Fabian 2004)).

1.2.3. Detection of Fe K and Fe L line emission

The presence of a strong reflection component in the relativistic reflection model is a natural consequence of having a X-ray corona close to the central black hole. In objects with high Fe to solar abundance values, which is the case for most Narrow-Line Seyfert 1 Galaxies, relativistic Fe K and Fe L lines have been detected. Fig. 3 shows the ratio of the data to a simple power law plus black body model (c.f. (Fabian et al. 2009) for details). Two unambiguous features appear between 0.6–1.0 keV and 4–7 keV. They are interpreted as broad Fe L and Fe K lines coming from the same medium with huge reflection fraction and high Fe abundance. It is important to note that the ratio in the photon flux between the two lines is 20 to 1, in agreement with atomic physics.

1.2.4. Detection of negative time lags

The detection of time lags between the primary power law photons and the reflection component is predicted by the relativistic reflection model and was first detected in 1H 0707–495 (Fabian et al. 2009). Fig. 4 shows the time lag between the primary power law component and the reflection component. At high frequencies, i.e. time scales larger than about 30 minutes, negative time lags are detected with a maximum of 30 seconds. The negative time lag is explained due to the longer travel time for the reflection component and is a crucial result further supporting the relativistic reflection model.

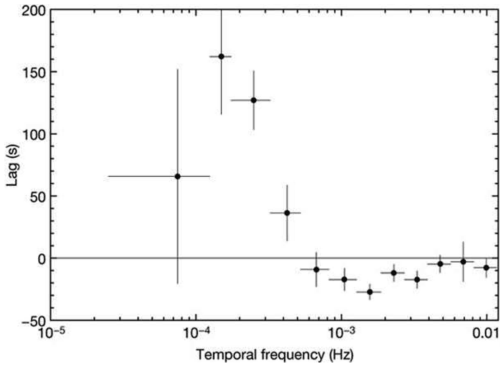

Fig. 4. Detection of negative time lags in 1H 0707–495 ((Fabian et al. 2009), their Fig. 3). Negative time lags are expected due to the longer travel time for the reflection component (Nature License Number 2900680198102).

1.3. Outer disc reflection and absorption

Alternative models to the inner disc reflection have been proposed by e.g. (Miller et al. 2010). The authors argue that their measured lags at soft, medium and high energy bands rule out model in which the inner accretion disc makes a significant contribution at both Fe L and Fe K energies. In particular, the lags between the hard and soft bands and between medium and soft bands are also negative. It is argued that the comparison between the observed lags and the lags predicted from the spectral model rules out the inner disc reflection model at larger than 99.9 percent confidence (c.f. their Fig. 3). The 1H 0707–495 data from (Fabian et al. 2009) have been reanalyzed by (Zoghbi et al. 2010) and the authors confirm their previous argumentation made in (Fabian et al. 2009) and argue that there are several problems with the outer disc reflection model, especially to explain the measured spectral complexity around 1 keV and the spectral and timing variability. In addition, an outer disc reflection model, associated with some significant outflowing disc wind, would result in strong absorption features, which are however not detected in 1H 0707–495. Such features are expected in sources with Super-Eddington accretion, which is the case for 1H 0707–495, due to strong outflowing winds with significant Thompson depths. The relation between Super-Eddington accretion and the parameters of the Comptonized outflow is described in part two of this paper.

2. AGN accretion states and their relation to Comptonized outflows

In the second part of this paper I relate the accretion states in AGN with their Comptonized outflows. In summary, I will show that the detailed relations might provide an explanation for the global X-ray Baldwin effect, which is the trend of decreasing X-ray luminosity with increasing UV luminosity density (Just et al. 2007).

2.1. The correlation between intrinsic spectral slope in X-rays and the amount of Compton reflection in AGN and Galactic binaries

It is well known that the amount of Compton reflection $\Omega/2\pi$ is strongly correlated with the X-ray power law photon index Γ. A natural explanation for the feedback is that the accretion disc emits soft photons which irradiate the plasma and results into Compton upscattering. The amount of Compton reflection is related to the amount of radiation-driven outflow from the AGN accretion disc which is a function of the accretion rate. The photon index is related to the rate of cooling by the incident soft UV photons arising from the accretion disc, c.f. Fig. 1 of (Zdziarksi et al. 1999).

A similar relation has been found by Gilfanov (c.f. his article in the proceedings) for Galactic black hole binaries.

2.2. Accretion rates and parameters of the Comptonized outflow

A more general picture can be derived when investigating the accretion rate in units of the Eddington ratio and the relation to the Comptonized outflow parameters. For a standard accretion disc and accretion below the Eddington ratio, no effective cooling of the plasma cloud is expected, the energy gain per inverse Compton scattering process is large, resulting into flat X-ray spectra and strong X-ray emission. For a Super-Eddington accretion rate the disc becomes optically and geometrically thick (Abramowicz et al. 1988). This results into strong radiation-driven outflows with significant Thompson depth values, a strong UV radiation field which cools down the plasma cloud. In addition photon trapping becomes important and as a result steep and weak X-ray spectra arise. The relation between the photon index, the optical depth and the dimensionless electron temperature Θ is $\Gamma = \ln \tau / \ln\,(1 + 4\Theta)$. It is obvious that in the case of Super-Eddington accretion steep X-ray photon indices arise as the optical depth in large and the dimensionless electron temperature of the plasma cloud is low.

The author of this paper has performed XMM-Newton simulations to quantify the relation between the accretion rate and the Comptonized plasma parameters more precisely. In Fig. 5 I show the spectral energy distribution from the optical to soft X-rays for (i) an accretion disc accreting 10 times above the Eddington limit, with a low electron temperature of the plasma cloud of 5 keV, (ii) a disc accreting at the Eddington limit with a plasma cloud temperature of 25 keV, and (iii) a disc accreting at 0.1 of the Eddington limit and a hot plasma cloud temperature of 50 keV. The stronger the UV emission, the weaker is the X-ray emission, which is exactly what is shown in Fig. 7 of (Just et al. 2007) and what is refereed to as the global X-ray Baldwin effect and what can generally be explained by the accretion state of the disc and the related parameters of the Comptonized outflow.

In (Boller et al. 2011) we analyzed an extreme example for the global X-ray Baldwin effect. The Narrow-Line Quasar LBQS 0102-2713 shows one of the highest Eddington ratios measured so far, ranging between about 5 and 50 times the Eddington ratio, an upper limit for the dimensionless electron temperature of the plasma cloud of 10 keV, and an extreme luminosity of $2{\times}10^{47}$ erg s^{-1}. The object might serve as a template for understanding the global X-ray Baldwin effect at large UV luminosity densities and large $\alpha_{\rm ox}$ values.

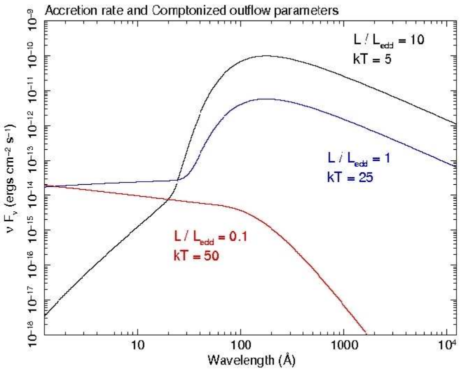

Fig. 5. XMM-Newton simulation for three states of the accretion rate and the related temperature of the Comptonizing plasma cloud. With the combination of both parameters the global X-ray Baldwin effect can be explained.

3. Summary

It is shown that the relativistic reflection model of (Ross & Fabian 2005) provides a solid spectral model to describe the X-ray spectra of AGN and that there is an excellent agreement between the model and the observations. In the second part of the review I have summarized that an increasing AGN accretion rate is related to (i) a stronger UV radiation, (ii) an increasing radiation-driven outflow, (iii) increasing reflection $\Omega/2\pi$, (iv) a stronger cooling of the plasma cloud, (v) steeper X-ray spectra and weaker X-ray emission, and, which qualitatively explains the global X-ray Baldwin effect.

4. Discussion

MAURI VALTONEN: Could you comment on the accuracy of the Galactic Center test of General Relativity at β^2 level, in particular in the quadrapole term.

THOMAS BOLLER: The expected spatial resolution for the β^2 effects as well as the lens-thirring precession is about 1 R_S.

KEN EBISAWA: We have analyzed Suzaku MCG-6-40-15 data to explain the spectral variation. Our model can explain the spectral variation only by the change of the partial covering fraction. The partial covering material has an inner ionization structure.

THOMAS BOLLER: I am aware that partial coverer models can also fit the data on steep spectrum AGNs, as I have shown in my first XMM-Newton publication on 1H 0707–495 in 2002. However, the light bending model gives a better physical description of the data. Especially significant absorption below 1 keV would be expected, which is however not seen in 1H 0707–495 and IRAS 13224–3809.
JÖRN WILMS: What do the χ^2 contours of r_{in} versus emissivity index look like?
THOMAS BOLLER: The fits are unique and the contour lines are closed and constrained.
GENNADI BISNOVATYI-KOGAN: The classical example of Super-Eddington accretion is the microquasar SS 433 with very specific features. It would be interesting to compare the properties of these two supercritical objects.
THOMAS BOLLER: I completely agree with that argumentation and there already some papers, e.g. (Boller 2010, AN 331, 235) in that respect. Having LBQS 0102–2713 as one of the highest AGN Eddington sources, the comparison with SS 433 is a hot topic to perform.

Acknowledgements. I am grateful to Marat Gilfanov for discussions on the reflection in AGN and Galactic binaries. I would like to thank my colleagues from the Scientific Organizing Committee for an effective preparing of the workshop and especially Franco Giovannelli for his longstanding efforts in leading the Vulcano workshops.

References

Abramowicz, M. A., Czerny, B., Lasota, J. P. et al. 1988, ApJ, 332, 646
Boller, Th., Fabian, A. C., Sunyaev et al. 2002, MNRAS, 329, 1
Boller, Th., Tanaka, Y., Fabian et al. 2003, MNRAS, 343, 89
Boller, Th., Schady, P., Heftrich, T. 2011, ApJ, 731, 16
Crummy, J., Fabian, A.C., Gallo, L., Ross, R.R., MNRAS 2006, 365, 1067
Fabian, A.C. et al. 2009, Nature 459, 540
Gallo, L., Tanaka, Y., Boller, Th. et al. 2004, MNRAS 353, 1064
Just, D. W., Brandt, W. N., Shemmer, O. et al. 2007, ApJ, 665, 1004
Miller, L., Turner, T. J., Reeves, J. et al. 2010, MNRAS, 408, 1928
Miniutti, G., Fabian, A.C. 2004, MNRAS 349, 1435
Ponti, G., Cappi, M., Vignali, C. et al. 2009, MNRAS, 394, 1487
Ross, R.R., Fabian, A.C. 2005, MNRAS 358, 211
Vaughan, S. & Fabian, A.C., 2004, MNRAS 348, 1415
Wilkins, D. R., Fabian, A. C. 2011, MNRAS 414, 1269
Zdziarski, A. A., Lubinski, P., Smith, D. A., 1999, MNRAS 303, L 11
Zoghbi, A., Fabian, A. C., Uttley, P. et al. 2010, MNRAS, 401, 2419